Chemical Engineering Journal 106 (2005) 261–267

Chemical Engineering Journal

www.elsevier.com/locate/cej

Supercritical water gasification of biomass: thermodynamic analysis with direct Gibbs free energy minimization

Huiqing Tang*, Kuniyuki Kitagawa

Division of Energy Science, Ecotopia Science Institute, Nagoya University, Furo-cho, Chikusa-ku, Nagoya 464-8603, Japan

Received 22 July 2004; received in revised form 15 November 2004; accepted 7 December 2004

Abstract

A thermodynamic model is developed to estimate equilibrium composition for supercritical water gasification (SCWG) of biomass. With a local optima solver and a global optima solver of LINGO, the algorithm based on Peng–Robinson EoS formulations and direct Gibbs free energy minimization can guarantee the convergence to the correct solution. Results are given for the supercritical water processes including supercritical water reforming of methanol, supercritical water gasification of glucose, catalyzed supercritical water gasification of cellulose and supercritical water gasification of real biomass. Model predictions are compared with various experimental measurements and the agreement is generally satisfying and therefore the correctness of the proposed model is demonstrated. Significant improvements of the comparison are obtained by analyzing reaction network and controlling steps of these processes and accounting them into calculation.

Keywords: Thermodynamic analysis; Biomass; SCWG; *PR* equation of state; Gibbs free energy minimization

1. Introduction

Whereas the use of hydrogen as a fuel for transportation and stationary application is receiving much attention as a technical and policy issue and also whereas the interest in renewable energy sources and utilization of various wastes and by-products are increasing, extracting hydrogen from biomass is under development. Among all the methods for gasifying biomass, supercritical water gasification (SCWG) has its advantages of high efficiency and adaptation to a broad range of biomass feedstock. So far most of work in this area has been focusing on experiment. Thermodynamic behavior of SCWG has not been systematically studied yet. In supercritical state, because of the equation of state of the mixture, the fugacity of each species is an extremely complicated function of pressure, temperature and mixture composition (e.g. molar fraction). Thermodynamic analysis of SCWG is beyond the ability of many existing equilibrium calculation packages. Hence to develop a comprehensive thermodynamic model for SCWG is necessary to meet the very need for analyzing reaction behavior and optimizing operation conditions.

Optimization techniques have been widely used for estimating equilibrium composition in chemical and phase equilibrium problems. Several papers have been published focusing on accurately determining the equilibrium composition and ensuring convergence of chemical and phase equilibrium problems [1–4]. Direct minimization of Gibbs free energy subject to the linear material balance constraints is reported to be very effective for complicated phase equilibrium and chemical equilibrium problems [5]. In this paper, we have formulated a thermodynamic model using direct Gibbs free energy minimization to predict the equilibrium composition of SCWG of biomass.

2. Model formulation

The first step in preparing the model is to estimate species in supercritical water gasification of biomass. Biomass gasification in supercritical water could be roughly summarized

* Corresponding author. Tel.: +81 52 789 3913; fax: +81 52 789 3910.
E-mail address: huiqingt@mail.apchem.nagoya-u.ac.jp (H. Tang).

1385-8947/$ – see front matter © 2004 Elsevier B.V. All rights reserved.
doi:10.1016/j.cej.2004.12.021

Nomenclature

a	Peng–Robinson temperature-dependent attraction parameter (N m^4/kmol^2)
a_m	mixture a (N m^4/kmol^2)
A^*	dimensionless form of a for a mixture
b	Peng–Robinson temperature-independent repulsion parameter (m^3/kmol)
b_m	mixture b (m^3/kmol)
B^*	dimensionless form of b for a mixture
fw	function of the acentric factor
G_i^0	Standard-state Gibbs free energy of the i-th species (J/mol)
k_{ij}	binary interaction coefficient between species i and j
n_i	number of moles of species i
n_{iT}	possible maximum of number of moles of species i
P	pressure (N/m^2)
P_{Ci}	critical pressure of species i (N/m^2)
P_0	standard-state pressure (N/m^2)
R	universal gas constant (kJ/kmol K, J/mol K)
T	temperature (K)
T_{Ci}	critical temperature of species i (K)
V	volume of the fluid mixture (m^3)
v	specific volume (m^3/kmol)
V_{Ci}	critical volume of species i (m^3/kmol)
x_i	molar fraction of species i
Z	compressibility factor

Greek symbols

β_{ej}	number of moles of element e in species j
β_e	total number of moles of element e in the system
ϕ_i	fugacity coefficient of species i
u_i	chemical potential of species i (J/mol)
w_i	acentric factor of species i

into three reactions:

$$CH_xO_y + (1-y)H_2O = CO + (x/2 + 1 - y)H_2 \quad (1)$$

$$CO + H_2O = CO_2 + H_2 \quad (2)$$

$$CO + 3H_2 = CH_4 + H_2O \quad (3)$$

There are still substances like C_2–C_3 hydrocarbons though their amounts are small.

And then, we have to choose an EoS to describe the thermodynamic behavior of each species in the SCWG system. In supercritical state, water has been found like a dense gas and has solvation properties resembling that of non-polar fluids [6]. This in turn leads to an increase of solubility of hydrocarbons and light gases in supercritical water and so the reacting system maybe assumed to be a single homogeneous fluid when it reaches equilibrium. In this paper, *PR* equation of state [7] is adopted not only for its wide application in the field of supercritical fluids, but for its usage by several researchers [8,9] to conduct their analysis of supercritical water reactions as well. For pure fluids, the *PR* state equation has the following function form:

$$P = \frac{RT}{v-b} - \frac{a(T)}{v^2 + 2bv - b^2} \quad (4)$$

The temperature-independent repulsion parameter b is:

$$b = \frac{0.07780RT_C}{P_C} \quad (5)$$

The temperature-dependent attraction parameter $a(T)$ is:

$$a(T) = a(T_C)\left[1 + fw\left(1 - \frac{T}{T_C}\right)^{0.5}\right]^2 \quad (6)$$

where

$$a(T_C) = \frac{0.45724R^2T_C^2}{P_C} \quad (7)$$

fw is correlated to the acentric factor w:

$$fw = 0.37464 + 1.54226w - 0.26992w^2 \quad (8)$$

To extend this EoS to mixture, Van der Waals one-fluid theory classical mixing rules is typically applied.

$$a_m = \sum_i \sum_j x_i x_j a_{ij} \quad (9)$$

$$b_m = \sum_i x_i b_i \quad (10)$$

$$a_{ij} = (a_i a_j)^{0.5}(1 - k_{ij}) \quad (11)$$

where k_{ij} is an additional interaction parameter, usually to be derived from experimental data if available, here it is estimated with the second virial coefficients of mixture following Eq. (12) as recommended by Prausnitz and Chueh [10] and Barragan et al. [11]:

$$k_{ij} = 1 - \frac{8(V_{Ci}V_{Cj})^{1/2}}{(V_{Ci}^{1/3} + V_{Cj}^{1/3})^3} \quad (12)$$

Introducing compressibility factor Z from Eq. (4), the *PR* equation of state can be rewritten as a third-order polynomial with Z appearing as the independent variable. The resulting expression is:

$$Z^3 - (1 - B^*)Z^2 + (A^* - 2B^* - 3B^{*2})Z - (A^*B^* - B^{*2} - B^{*3}) = 0 \quad (13)$$

where

$$A^* = \frac{a_m(T)P}{R^2T^2}$$

$$B^* = \frac{b_mP}{RT}$$

Table 1
Physical properties used in calculation

Substance	Formula	Molecular weight	Critical temperature (K)	Critical pressure (MPa)	Critical volume (m^3/kmol)	Acentric factor
Glucose[a]	$C_6H_{12}O_6$	180	1011.0	6.20	0.416	2.547
Methanol	CH_3OH	32	513.2	7.85	0.188	0.556
Water	H_2O	18	647.3	22.00	0.056	0.348
Carbon dioxide	CO_2	44	304.2	7.39	0.094	0.420
Carbon monoxide	CO	28	133.0	3.50	0.093	0.041
Hydrogen	H_2	2	33.0	1.30	0.064	0.000
Methane	CH_4	16	191.1	4.58	0.099	0.013
Ethane	C_2H_6	30	305.4	4.82	0.148	0.105
Propane	C_3H_8	44	369.9	4.20	0.200	0.152
Ethylene	C_2H_4	28	283.1	5.05	0.124	0.073
Propene	C_3H_6	42	225.5	4.54	0.181	0.143

[a] Estimation from ref. [12].

Calculation of the thermodynamic definition for ϕ_i, partial fugacity coefficient of species i, follows:

$$\phi_i = \frac{1}{Z}\exp\left(\frac{1}{RT}\int_V^\infty \left[\frac{\partial P}{\partial n_i}|_{T,V,n_{j(j\neq i)}} - \frac{RT}{V}\right]\mathrm{d}V\right) \quad (14)$$

Based on the above mixing rule and compressibility factor Z, the fugacity coefficient of component i in the fluid mixture could be simplified as:

$$\ln\phi_i = \frac{b_i}{b_m}(Z-1) - \ln(Z-B^*) - \frac{A^*}{2B^*\sqrt{2}} \times \left(\frac{2\sum_j x_j a_{ij}}{a_m} - \frac{b_i}{b_m}\right)\ln\left(\frac{Z+(1+\sqrt{2})B^*}{Z+(1-\sqrt{2})B^*}\right) \quad (15)$$

and the chemical potential of species i is:

$$u_i = RT\left[\ln\left(\frac{\phi_i P}{P_0}\right) + \ln(X_i) + G_i^0(T, P_0)\right] \quad (16)$$

Gibbs free energy function G of the system is expressed as a linear combination of chemical potential of each component in the system:

$$G = \sum_i^{i=K} n_i\mu_i \quad (17)$$

At last, chemical potential is expressed in terms of the Gibbs free energy of formation and fugacity. So Eq. (17) can be rewritten as:

$$G = \sum_i^{i=K} n_i\left[RT\left(\ln\left(\frac{\phi_i P}{P_0}\right) + \ln(X_i)\right) + G_i^0(T, P_0)\right] \quad (18)$$

Under given temperature and pressure, at equilibrium, G should be global minimum with n_i satisfying elemental mass balance and non-negativity requirements. For chemical equilibrium in a single phase, the conservation of moles of individual component must hold:

$$\sum_i^k \beta_{ei} n_i = \beta_e \qquad (e = 1, 2, 3 \ldots M) \quad (19)$$

The bounds on variables are:

$$0 \le n_i \le n_{iT} \qquad (i = 1, 2, 3, \ldots, K) \quad (20)$$

Thus, to obtain equilibrium composition at equilibrium, it is necessary to find the global minimum of Gibbs free energy

Table 2
Enthalpy, entropy and heat capacity of components at the reference state

Component	T (K)	C_p (J/mol K)	H_0 (kJ/mol)	S_0 (J/mol K)
Glucose (i.g)[a]	298–1000	$176.667 + 406.843E-3T - 59.818E5T^{-2} - 151.538E-6T^2$	−1256.9	268.230
Methanol (g)	298–1000	$6.448 + 123.759E-3T + 3.686E5T^{-2} - 41.116E-6T^2$	−201.167	239.810
H_2O (g)	298–600	$33.570 - 4.20E-3T + 14.760E-6T^2$	−241.826	188.834
	600–1600	$21.870 + 22.560E-3T - 8.490E5T^{-2} - 4.00E-6T^2$		
CO (g)	298–3000	$25.694 + 8.293E-3T + 1.109E5T^{-2} - 1.477E-6T^2$	−110.541	197.661
CO_2 (g)	298–3000	$42.388 + 15.100E-3T - 8.891E5T^{-2} - 2.908E-6T^2$	−393.505	213.769
H_2 (g)	298–400	$16.920 + 61.459E-3T + 0.590E5T^{-2} + 79.559E-6T^2$	0.0	130.679
	400–1600	$28.280 + 0.418E-3T + 0.820E5T^{-2} - 1.469E-6T^2$		
CH_4 (g)	298–3000	$12.447 + 76.689E-3T + 1.448E5T^{-2} - 18.004E-6T^2$	−74.863	186.213
C_2H_6 (g)	298–1100	$10.297 + 160.912E-3T - 1.268E5T^{-2} - 48.212E-6T^2$	−84.684	229.601
C_3H_8 (g)	298–1100	$13.803 + 242.793E-3T - 4.669E5T^{-2} - 80.521E-6T^2$	−103.926	269.663
C_2H_4 (g)	298–2000	$29.790 + 84.977E-3T - 9.657E5T^{-2} - 20.535E-6T^2$	52.467	219.334
C_3H_6 (g)	298–1800	$5.113 + 227.656E-3T + 8.636E5T^{-2} - 84.295E-6T^2$	53.220	238.011

[a] Estimation from ref. [12].

as given by Eq. (18) subject to the constraints imposed by Eqs. (19) and (20).

The availability of thermodynamic data varies from species to species. In this paper, thermodynamic data and critical properties of glucose are from ref. [12] and necessary data of other components from HSC 2.0 thermodynamic database and ref. [13]. The thermodynamic data and critical properties of all substances are listed in Tables 1 and 2.

3. Model implementation

We have chosen to treat this optimization problem as one of constrained optimizations, retaining Eq. (19) as constraints rather than using them to eliminate variables. This increases problem size but leaves it well within the capacity of the available optimization packages. The direct search optimization procedure includes a local optima solver and a global optima solver, the local optima solver adopts a combination of generalized reduced gradient (GRG) [14] and method of approximation programming (MAP or SLP) [14] algorithms. The global solver adopts a series of range bounding and range reduction techniques within a branch-and-bound framework, which could be referred to tunneling global optimization [5]. These two solvers, as a DLL from LINGO, are incorporated into our own program. Because Z cannot be explicitly expressed with T, P and mixture composition through Eq. (13), the convergence of compressibility factor Z and global minimum searching are performed in two stages. The detailed numerical procedure could be summarized as follows:

(1) Choose an initial point: For computational efficiency, improved estimation is necessary.
(2) Calculate the compressibility factor with Eq. (13).
(3) Implement non-linear local solver and global solver to search the equilibrium point.
(4) Repeat steps (2) and (3) until Z reaches convergence.
(5) Interpret the result.

4. Results and discussion

The proposed model has been applied to analyze supercritical water reforming of methanol, supercritical water gasification of glucose, cellulose and real biomass. We have not met any numerical difficulties except for long CPU time in some cases, which means the model is robust and versatile.

4.1. Methanol

We analyzed supercritical water reforming of methanol in a compact reformer and compared the results to the work of Taylor et al. [15]. Numerical results showed, in all cases, that the equilibrium molar fraction of methanol was usually less than 1.0E-6 and thus was negligible. We plotted in Fig. 1 the molar fractions of substantial gaseous species as a function of feed methanol concentration. From Fig. 1, it is observed that an increase in feed methanol concentration causes a decrease of hydrogen composition at a given temperature and a given pressure. By contrast, it favors the formation of methane. We plotted in Fig. 2 the molar fractions of substantial gaseous species as a function of temperature. From Fig. 2, it is observed that an increase of temperature causes an increase of hydrogen composition while a decrease of methane composition. In Figs. 1 and 2, the present calculations are in poor agreement with the experimental measurements, especially as feed methanol concentration increases or temperature decreases. The reaction pathway of supercritical water reforming of methanol proposed by Taylor is that methanol firstly decomposes to hydrogen and carbon monoxide and then CO_2 and CH_4 are formed through water-gas shift reaction (reaction (2)) and methanation reaction (reaction (3)). Taylor indicated that the inconel 625, of which the compact reformer used in his work was made, appeared to catalyze the water-gas shift reaction and to suppress the methanation reaction. Because of these two reasons and the short reactor residence

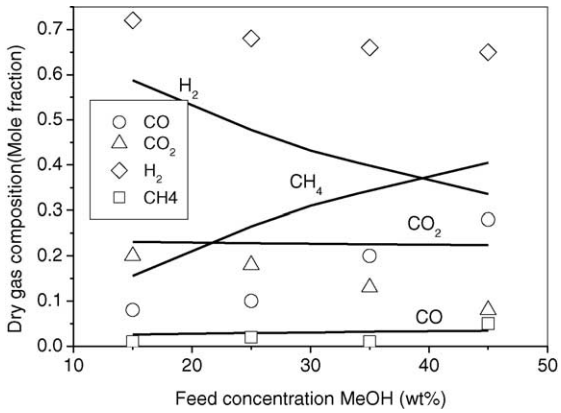

Fig. 1. Supercritical water reforming of methanol: Comparison of experimental data with calculations, development with feed concentration of methanol (T: 973 K; P: 27.6 MPa; line: equilibrium; symbol: experimental data (residence time: 6 s) [15]).

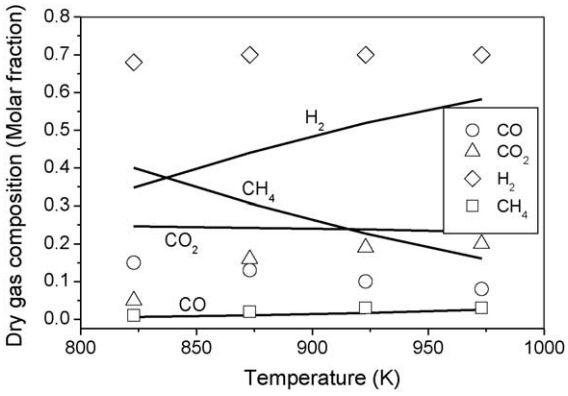

Fig. 2. Supercritical water reforming of methanol: Comparison of experimental data and calculations, development with different temperature (feed concentration: 15 wt.%; P: 27.6 MPa; line: model prediction; symbol: experimental data (residence time 6 s) [15]).

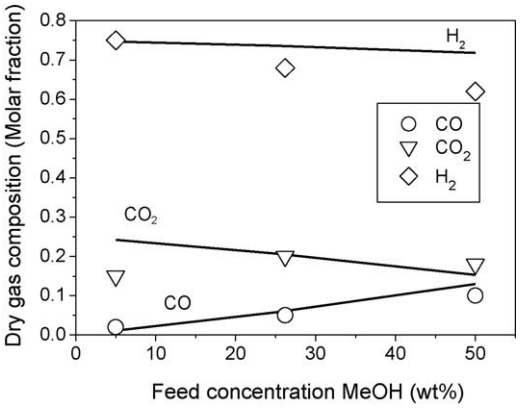

Fig. 3. Supercritical water reforming of methanol: Comparison of experimental data with calculations, development with methanol feed concentration (CH_4 excluded) (T: 873 K; P: 25 MPa; line: model prediction; symbol: experimental data (mean residence time 45 s) [16]).

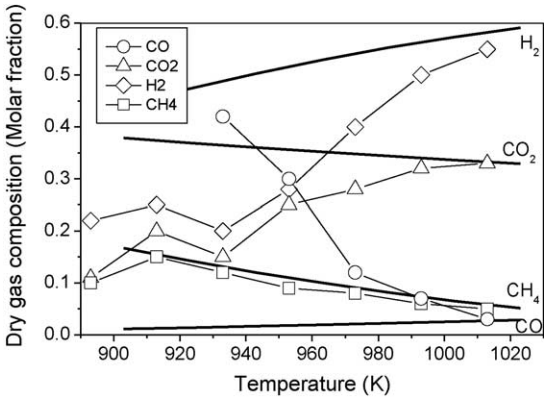

Fig. 4. Supercritical water gasification of glucose: Comparison of experimental data with calculations, development with temperature (feed concentration: 0.6 M glucose; P: 28 MPa; line: model prediction; symbol: experimental data [18]).

time (6 s), the proposed model tends to underpredict the molar fraction of hydrogen and overpredict the molar fraction of methane.

We therefore compared our model predictions to the work of Boukis et al. [16]. The experiment runs were chosen with a residence time of some 45 s which could assure complete conversion of methanol. In this case, we dropped methane in our calculations for methane in the gas product was ignored in both the work of Taylor et al. and that of Boukis et al. The comparison is shown in Fig. 3. In Fig. 3, model predictions could fit the experiment measurements quite well. This indicates that methanation reaction (reaction (3)) is a very slow step in supercritical water methanol reforming.

4.2. Glucose

We analyzed glucose gasification in supercritical water then. Glucose could be seen as a monomer of cellulose and gasification of glucose can be considered as a good model for gasification of more complex cellulosic biomasses in supercritical water [17]. We analyzed the influence of the temperature on glucose gasification in supercritical water. Results of calculation were compared to the work of Lee and Kim [18]. In Lee's work, the gas product still included C_2H_4, C_2H_6, C_3H_6, and C_3H_8 and therefore we performed calculations considering all these components. However, equilibrium molar fractions of these C2–C3 hydrocarbons were still negligibly small ($<10^{-5}$) and so we did not take them into our final analysis. Numerical results also showed that glucose could be completely decomposed under supercritical condition. We plotted in Fig. 4 variations of major gas compositions as a function of temperature. As can see from Fig. 4, it is clear that experiment measurements of hydrogen and carbon dioxide fall well below their respective equilibrium lines while those of carbon monoxide are well above its equilibrium line. But in the temperature range above 973 K, the fitness becomes satisfying.

As reported by Lee et al., the gasification efficiency of glucose was low with a reactor residence time of 30 s and at low temperature, which is reflected in Fig. 5. We consequently assumed the gasification of glucose included the following steps:

$$\text{Glucose} \rightarrow \text{CO} + \text{H}_2 + \text{CH}_4 + \text{H}_2\text{O} \quad (21)$$

$$\text{CH}_4 + \text{H}_2\text{O} = \text{CO} + 3\text{H}_2 \quad (22)$$

Sato et al. [19] reported that water-gas shift reaction (reaction (2)) was very slow at temperature below 873 K and we neglected it in our subsequent calculations. We still accounted the destruction efficiency of COD (Fig. 5) directly as gasification efficiency of glucose into our calculations. Comparison of the calculation results to the experimental measurements is shown in Fig. 7. It is clear that the fitness in Fig. 6 is much better than that in Fig. 4 at temperature below 900 K.

This comparison indicates the gasification pathway of glucose is different from that of methanol reforming. Calculations still indicate that, at low temperature, glucose gasification does not consume water but could contribute water. Calculation results of yield of water generated from glucose decomposition versus temperature are shown in Fig. 7. From Fig. 7, the gasification of glucose reaction (21) might be

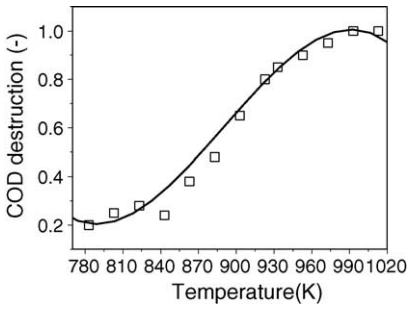

Fig. 5. COD destruction efficiency vs. reaction temperature [18] (feed concentration: 0.6 M glucose; P: 28 MPa; reactor residence time: 30 s).

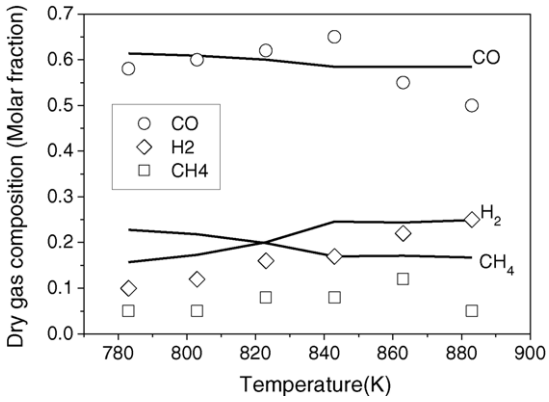

Fig. 6. Supercritical water gasification of glucose: Comparison of experimental data with calculations, development with temperature (CO_2 excluded) (feed concentration: 0.6 M; *P*: 28 MPa; line: model prediction; symbol: experimental data [18]).

envisaged as:

$$2C_6H_{12}O_6(COD) = 9CO + 3H_2 + 3CH_4 + 3H_2O \quad (23)$$

Under temperature from 873 to 973 K, reaction (2) becomes prominent to determine the final species compositions of glucose gasification. At temperature above 973 K, the system could reach equilibrium in a short time as reflected in Fig. 4.

4.3. Cellulose

Cellulose (represented as $C_6H_{10}O_5$) is a polymer and its thermodynamic data for calculation is unavailable. But however cellulose could be completely converted to glucose and oligomers at temperature above 673 K in supercritical water [20]. The above analysis of methanol reforming and glucose gasification also informs us that cellulose could be assumed to be completely destroyed in SCWG. Since the proposed model is based on molar composition, we have only to know the numbers of mole of carbon, hydrogen and oxygen atoms in the initial state.

Several researchers have conducted cellulose gasification in supercritical water with various catalysts including bases (NaOH, KOH etc.), ZrO_2, reduced nickel particles and so on

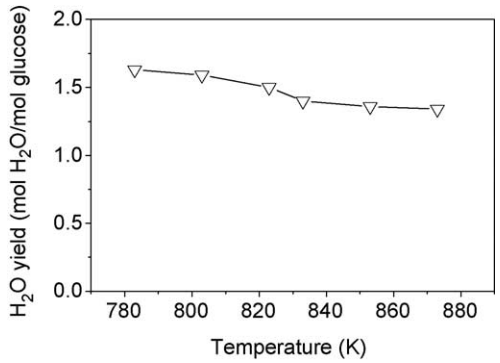

Fig. 7. Supercritical water gasification of glucose: Yield of water vs. temperature (feed concentration: 0.6 M glucose; *P*: 28 MPa).

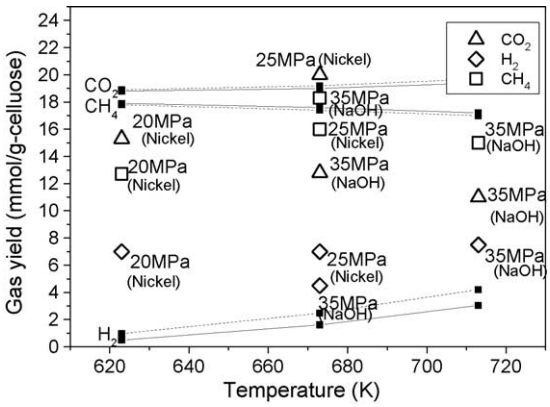

Fig. 8. Catalyzed supercritical water gasification of cellulose: Comparison of experimental data with calculations development with temperature (feed concentration: 14 wt.% cellulose; solid line: predicted value under 35 MPa; dash line: predicted value under 25 MPa; symbol: experimental data [20–24]; compound: catalyst used in experiment).

[21–24]. All these work on cellulose gasification were carried out under relatively low temperature (623–713 K). Catalysts can promote the reaction rate while cannot change the equilibrium. Here we only selected some experiment measurements with cellulose conversion more than 90% and feed cellulose concentration 8 through 14 wt.% to validate our model. Comparison of calculations to experiments is given in Fig. 8.

In the above section of glucose gasification, the analysis indicates that there is a large amount of CO in the gas product if CO_2 is excluded. Here, calculations showed the equilibrium CO yield was very small (<0.05 mmol/g cellulose in all cases). Though the reaction system can not reach equilibrium in a short time even with various catalysts, the major compounds (CH_4, CO_2, and H_2) fall near to their respective equilibrium lines as can be seen from Fig. 8. A comparison of Figs. 6–8 indicates that these catalysts could promote the water-gas shift reaction and the methanation reaction efficiently.

We still analyzed the influence of pressure on cellulose gasification. In Fig. 8, it may be observed that increasing pressure does not change the general shape of the diagram. The effect of pressure on major species yields is far less than that of temperature.

Model predictions showed that major products of cellulose gasification were methane and CO_2, which is shown in Fig. 8. This means that low temperature does not favor the formation of hydrogen.

4.4. Real biomass

Real biomass includes municipal solid wastes and agricultural resources. The main components of biomass are C, H, and O which account for more than 98 wt.% (dry basis). Based on the aforementioned analysis of methanol, glucose, and cellulose, calculations were performed to the real biomass of starch and sawdust in a similar method as that with cellulose. We selected some tabulated experimental tests

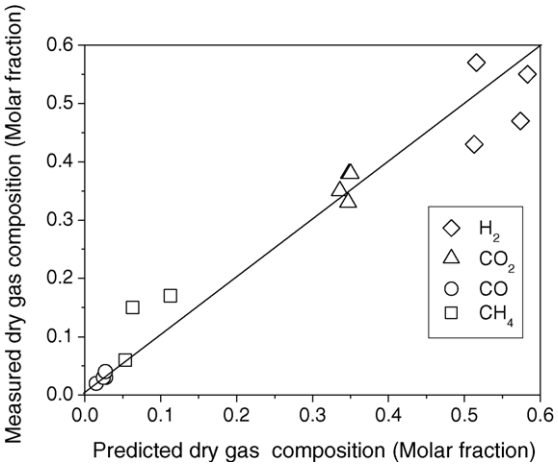

Fig. 9. Supercritical water gasification of real biomass: Comparison of experimental data with calculations (feed concentration: 10–15 wt.% biomass; *P*: 28 MPa; experimental data from ref. [25]).

from Tables 2 and 3 of the work of Antal et al. [25] for validation of the proposed model. The calculations were limited to temperature above 923 K, feed concentration of biomass 10–15 wt.% and mass flow rate 1.0–4.0 g/min for the analysis of methanol, glucose, and cellulose showed that temperature and initial feed concentration play very important roles on SCWG of biomass. The comparison of the model predictions to the experiment measurements is shown in Fig. 9. As can see from Fig. 9, the agreement is surprisingly good.

5. Conclusion

Chemical equilibrium of supercritical water gasification of biomass can be modeled through the use of the general-purpose non-linear programming algorithm. The model developed with Peng–Robinson EoS and global Gibbs free energy minimization strategy is successfully applied to analyze processes including supercritical water reforming of methanol, supercritical water gasification of glucose, cellulose, and real biomass. The results have been validated and analyzed. Significant improvements of fitness between model predictions and experiment measurements have been obtained by accounting reaction networks and rate controlling steps of these processes into calculations. The present work indicates the proposed model is an attractive means for analyzing supercritical water gasification of biomass.

References

[1] C.M. Mcdonald, D.A. Flaucas, Global optimization for the phase and chemical equilibrium problem: application to NTRL equation, Comput. Chem. Eng. 19 (1995) 1111–1139.
[2] J.M. Reneaume, M. Meyer, J.J. Letourneau, X. Joulia, A global MINLP for phase equilibrium calculations, Comput. Chem. Eng. 20 (1996) 303–308.
[3] Y. Sofyan, A.J. Ghaja, K.A.M. Gasem, Multiphase equilibrium calculations using Gibbs minimization techniques, Ind. Eng. Chem. Res. 42 (2003) 3786–3801.
[4] S. Chaikunchuensakun, L.I. Stiel, A combined algorithm for stability and phase equilibrium by Gibbs free energy minimization, Ind. Eng. Chem. Res. 41 (2002) 4132–4140.
[5] V.D. Nichita, S. Gomez, E. Luna, Multiphase equilibria calculation by direct minimization of Gibbs free energy with a global optimization method, Comput. Chem. Eng. 26 (2002) 1073–1724.
[6] N. Akiya, E.P. Savage, Roles of water for chemical reactions in high temperature water, Chem. Rev. 102 (2002) 2725–2750.
[7] A.L. Muhlbauer, J.D. Raal, Computational and thermodynamic interpretation of high-pressure vapour–liquid equilibrium—a review, Chem. Eng. J. 60 (1995) 1–29.
[8] W. Feng, H. Kooi, J. Arons, Phase equilibria for biomass conversion processes in subcritical and supercritical water, Chem. Eng. J. 98 (2004) 105–113.
[9] M.K. Alkam, V.M. Pai, P.B. Butler, W.J. Pitz, Methanol and hydrogen oxidation kinetics in water at supercritical states, Combust. Flame 106 (1996) 110–130.
[10] J.M. Prausnitz, P.L. Chueh, Computer Calculations for High-Pressure Vapor–Liquid Equilibria, Prentice-Hall, 1968, pp. 58–59 (Prentice-Hall International Series in the Physical and Chemical Engineering Sciences).
[11] M. Barragan, S. Woods, H.L. Julien, Thermodynamic equation of state for hydrazine and monomethylhydrazine, Combust. Flame 131 (2002) 316–328.
[12] J.R. Wooley, V. Putsche, Development of an ASPEN PLUS physical property database for biofuel components, Report of National renewable energy laboratory (U.S.), April, 1996.
[13] R.C. Reid, T.K. Sherwood, The Properties of Gases and Liquids, second ed., McGraw Book Company, NY, 1966.
[14] D.M. Himmelblau, Applied Nonlinear Programming, McGraw-Hill Book Company, New York, 1972, pp. 274–289.
[15] J.D. Taylor, M.H. Christopher, B.C. Wu, K. Wally, S.F. Rice, Hydrogen production in a compact supercritical reformer, Int. J. Hydrogen 28 (2003) 1171–1178.
[16] N. Boukis, V. Diem, W. Habicut, E. Dinjus, Methanol reforming in supercritical water, Ind. Eng. Chem. Res. 42 (2003) 728–735.
[17] B.M. Kabyemela, T. Adschiri, R.M. Malaluan, K. Arai, Glucose and fructose decomposition in subcritical and supercritical water: detailed reaction pathway, mechanisms, and kinetics, Ind. Eng. Chem. Res. 38 (1999) 2888–2895.
[18] I. Lee, M. Kim, Gasification of glucose in supercritical water, Ind. Eng. Chem. Res. 41 (2002) 1182–1188.
[19] T. Sato, S. Kurosawa, L.R. Smith, et al., Water-gas shift reaction kinetics under noncatalytic conditions in supercritical water, J. Supercrit. Fluids 29 (2004) 113–119.
[20] M. Sasaki, T. Adschiri, K. Arai, Kinetics of cellulose conversion at 25 MPa in sub- and supercritical water, AIChE J. 50 (2004) 192–202.
[21] T. Yoshida, Y. Oshima, Y. Matsumura, Gasification of biomass model compounds and real biomass in supercritical water, Biomass Bioenergy 26 (2004) 71–78.
[22] T. Minowa, F. Zhen, T. Ogi, Cellulose decomposition in hot compressed water with alkali or nickel catalyst, J. Supercrit. Fluids 13 (1998) 253–259.
[23] T. Minowa, S. Inoue, Hydrogen production from biomass by catalytic gasification in hot compressed water, Renewable Energy 16 (1999) 1114–1117.
[24] M. Watanbe, H. Inomata, K. Arai, Catalytic hydrogen generation from biomass (glucose and cellulose) with ZrO_2 in supercritical water, Biomass Bioenergy 22 (2002) 405–410.
[25] M.J. Antal Jr., S.G. Allen, D. Schulman, X. Xu, Biomass gasification in supercritical water, Ind. Eng. Chem. Res. 39 (2000) 4040–4053.